Supplementary

Article

Elastic Nanofibrous Membranes for Medical and Personal Protection Applications: Manufacturing, Anti-COVID-19, and Anti-Colistin Resistant Bacteria Evaluation

Latifah Abdullah Alshabanah [1,†], Nada Omran [2, 3,†], Bassma H. Elwakil [4], Moaaz T. Hamed [5], Salwa M. AbdAllah [6], Laila A. Al-Mutabagani [1], Dong Wang [7], Qiongzhen Liu [8], Nader Shehata [3,9,10,11], Ahmed H. Hassanin [3,12,13] and Mohamed Hagar [14,15,*]

1 Chemistry Department, College of Science, Princess Nourah Bint Abdulrahman University, Riyadh 11671, Saudi Arabia; laalsabanah@pnu.edu.sa (L.A.A.); laalmutbagani@pnu.edu.sa (L.A.A.-M.)
2 Science and Technology Institute, Wuhan Textile University, Wuhan 430073, China; nada.omranplus@gmail.com
3 Centre of Smart Nanotechnology and Photonics (CSNP), SmartCI Research Centre, Alexandria University, Alexandria 21544, Egypt; nader83@vt.edu (N.S.); ahassanin2003@yahoo.com (N.S.);
4 Department of Medical Laboratory Technology, Faculty of Applied Health Sciences Technology, Pharos University in Alexandria, Alexandria21321, Egypt; bassma.hassan@pua.edu.eg
5 Industrial Microbiology and Applied Chemistry Program, Department of Botany & Microbiology, Faculty of Science, Alexandria University, Alexandria 21568, Egypt; moazt258@gmail.com
6 Materials Science & Engineering Department, School of Innovative Design Engineering, Egypt-Japan University of Science and Technology (E-JUST), New Borg El-Arab City, Alexandria 21934, Egypt; salwaabdallah17@gmail.com
7 Key Laboratory of Textile Fiber and Products (Ministry of Education), Wuhan Textile University, Wuhan 430200, China; wangdon08@126.com
8 Hubei Key Laboratory of Advanced Textile Materials & Application, Hubei International Scientific and Technological Cooperation Base of Intelligent Textile Materials & Application, Wuhan Textile University, Wuhan 430200, China; windlqz_2000@163.com
9 Department of Engineering Mathematics and Physics, Faculty of Engineering, Alexandria University, Alexandria 21544, Egypt
10 USTAR Bioinnovations Centre, Faculty of Science, Utah State University, Logan, UT 84341, USA
11 Department of Physics, School of Engineering, Kuwait College of Science and Technology (KCST), Doha Superior Rd., Jahraa 13133, Kuwait
12 Materials Science & Engineering Department, School of Innovative Design Engineering, Egypt-Japan University of Science and Technology (E-JUST), 179 New Borg El-Arab City, Alexandria 21934, Egypt

[13] Department of Textile Engineering, Faculty of Engineering, Alexandria University, Alexandria 21544, Egypt
[14] Chemistry Department, Faculty of Science, Alexandria University, Alexandria 21321, Egypt
[15] Chemistry Department, College of Sciences, Yanbu, Taibah University, Yanbu 30799, Saudi Arabia
* Correspondence: Mohamed.Hagar@alexu.edu.eg
† authors contributed equally to this work.

Transmission Electron Microscope Images (TEM)

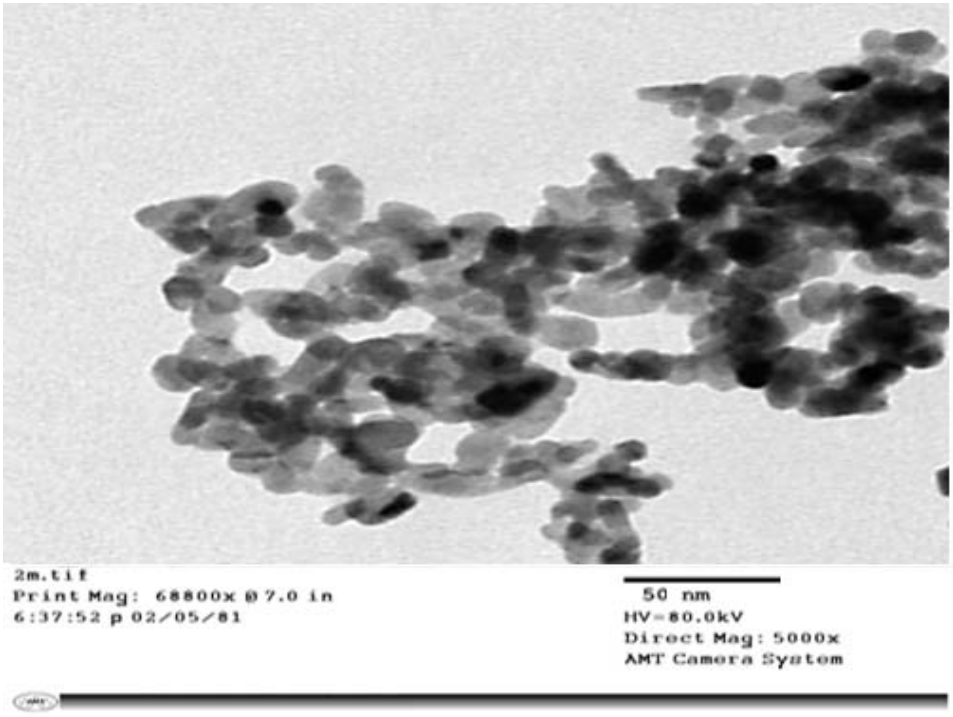

Figure S1: TEM micrographs of ZnO NPs

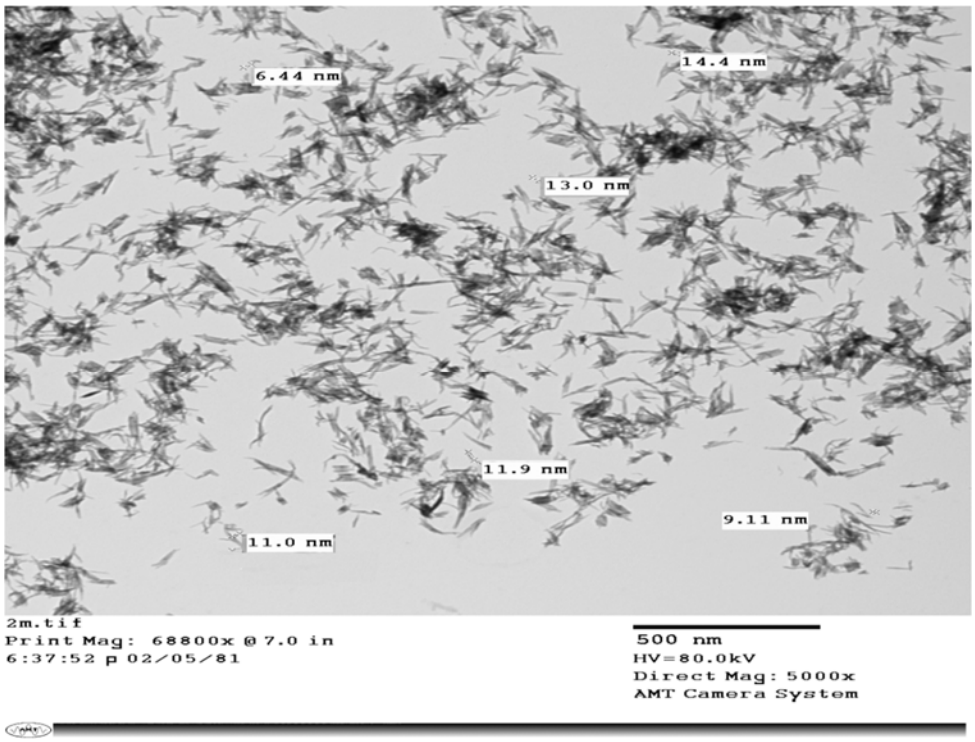

Figure S2: TEM micrographs of CuO NPs

SEM analysis:

The SEM images of ZnO samples show that the agglomerations of particles occur much less in this method of preparation.

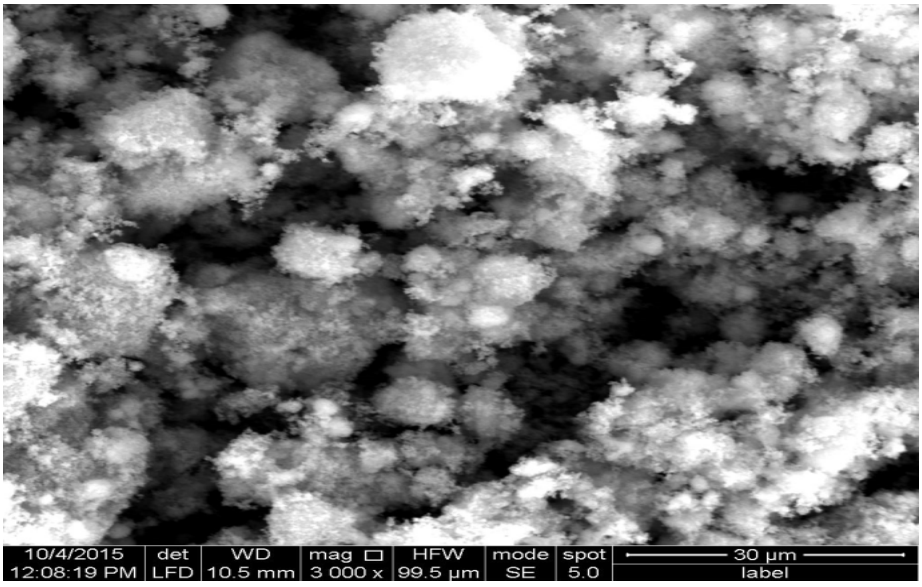

Figure S3: SEM micrographs of ZnO NPs

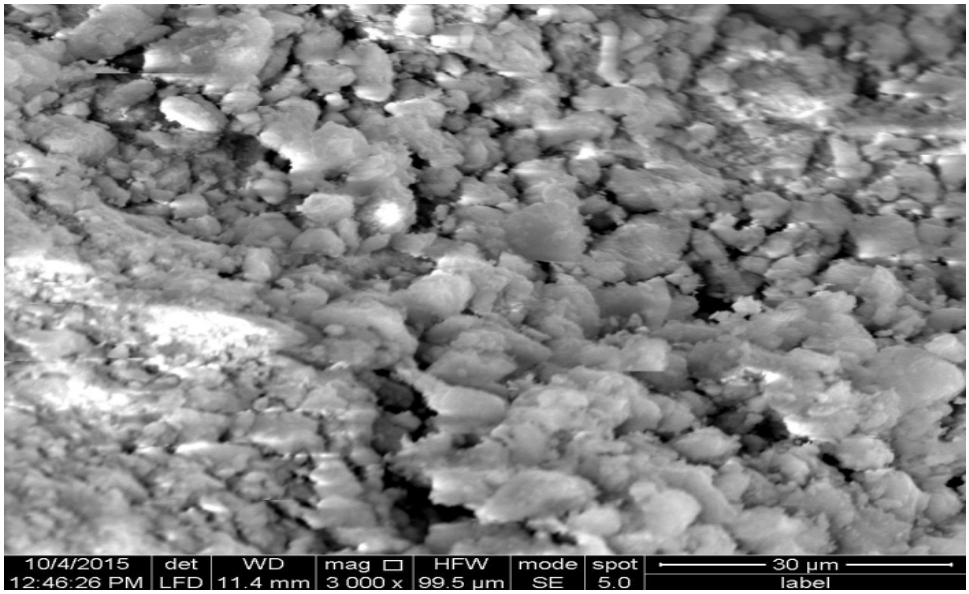

Figure S4: SEM micrographs of CuO NPs

X-ray Diffractometer Analysis:

XRD pattern of ZnO NPs indicated only characteristic peaks for crystalline ZnO hexagonal phase at (31.74^{o}, 34.42^{o}, 36.24^{o}, 47.5^{o}, 56.62^{o}, 62.83^{o}, 66.4^{o}, 67.93^{o}, and 69.05^{o}), respectively, were indexed to (100), (002), (101), (102), (110), (103), (200), (112), and (201) planes. All the diffraction peaks are well indexed to the hexagonal ZnO wurtzite structure (JCPDS no. 36–1451). Diffraction peaks corresponding to the impurity were not found in the XRD patterns, confirming the high purity of the synthesized products.

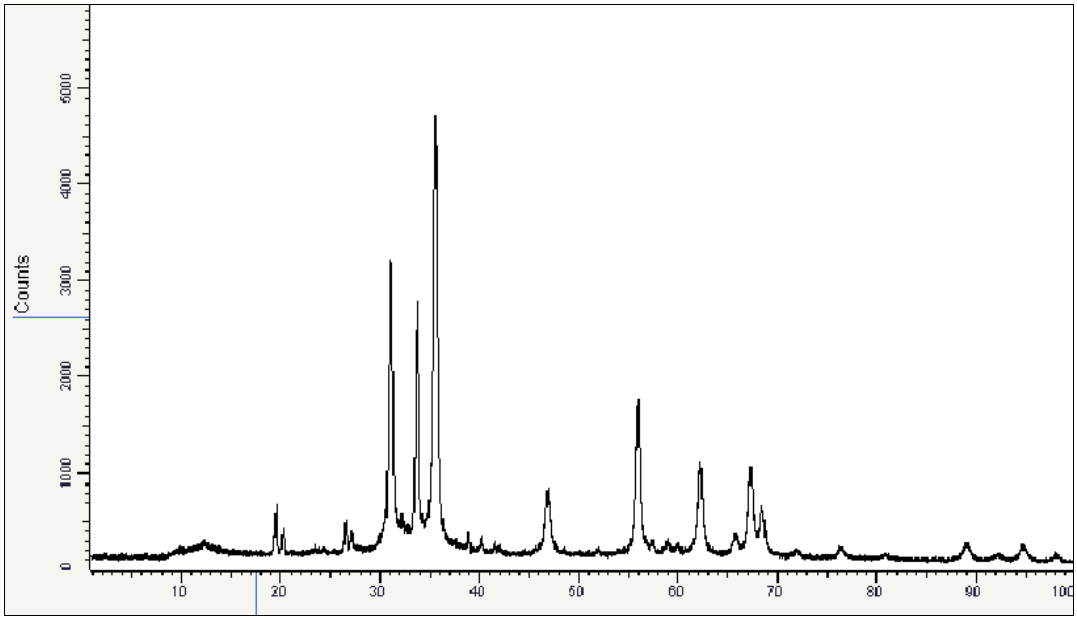

Figure S5: XRD pattern of ZnO NPs

Crystalline nature of the prepared CuO nanoparticles was identified from their corresponding powder XRD patterns (Figure S5). All the diffractions were well matched with monoclinic phase of CuO (standard JCPDS File No: 048-1548). Diffraction peaks with 2Θ 33.6°, 35.45°, 38.73°, 48.92°, 61.99°, and 66.49°, respectively, were indexed to (110), (002), (111), (020), (022), and (113) planes.

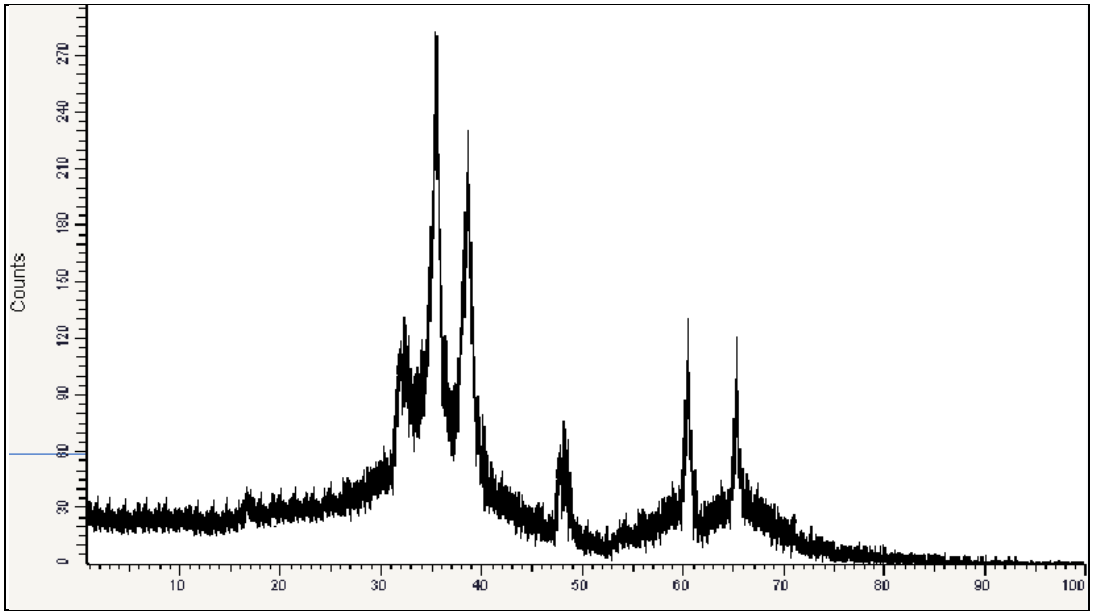

Figure S6: XRD pattern of CuO NPs.

1.5- FT-IR spectroscopy Analysis:

Figure S7 showed the FTIR spectra of ZnO nanoparticles. Metal oxides generally give absorption bands in finger print region, i.e., below 1000 cm^{-1} arising from inter-atomic vibrations. The peak at 1388.70 cm^{-1} and 1507.80 cm^{-1} corresponds to C=O and C–O bending vibrations, respectively .The peak observed at 3366.35 and 1036.07 cm^{-1} are may be due to O–H stretching and deformation, respectively assigned to the water adsorption on the metal surface.

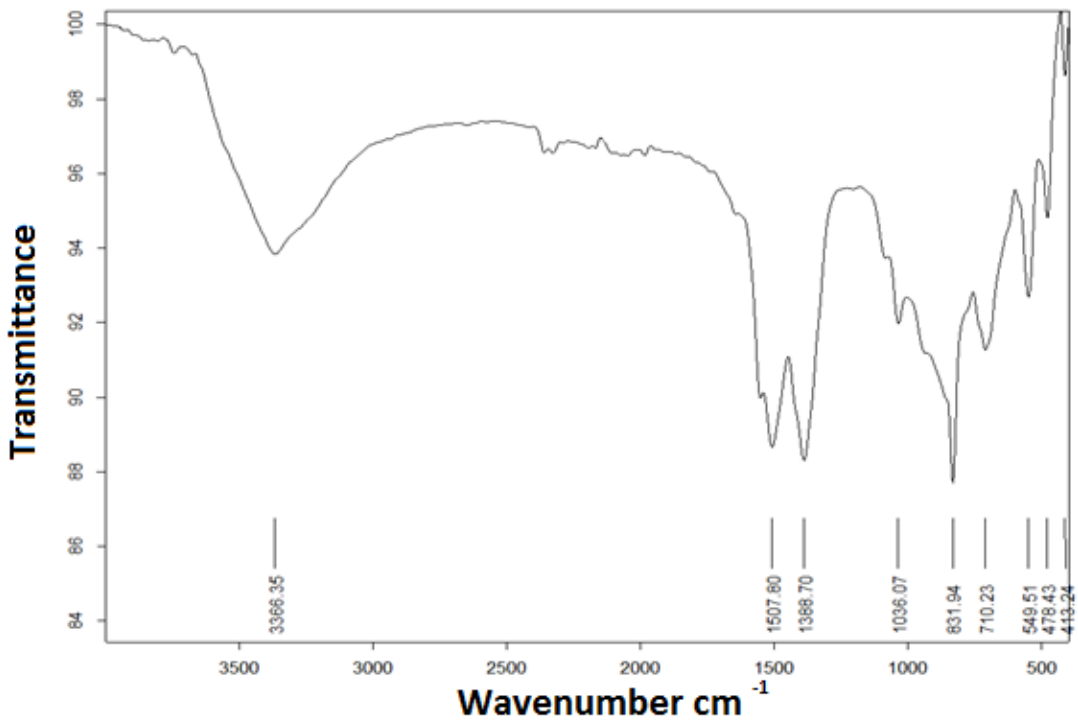

Figure S7: FTIR spectra of the ZnO NPs.

Figure S8 showed the FTIR spectra of CuO-NPs. The broad absorption peak at 3390 cm^{-1} was caused by the adsorbed water molecules. Since the nano crystalline materials possess a high surface to volume ratio, they can absorb moisture. The peaks at 1633 may be for the Cu–O symmetrical stretching. The high-frequency mode at 605.05 cm^{-1} and 490.60 cm^{-1} can be assigned to the Cu-O stretching vibration. Moreover, no other IR active mode was observed in the range of 605 to 660 cm^{-1}, which totally rules out the existence of another phase, i.e., Cu_2O. Thus, the pure phase CuO with monoclinic structure is also confirmed from the FTIR analysis.

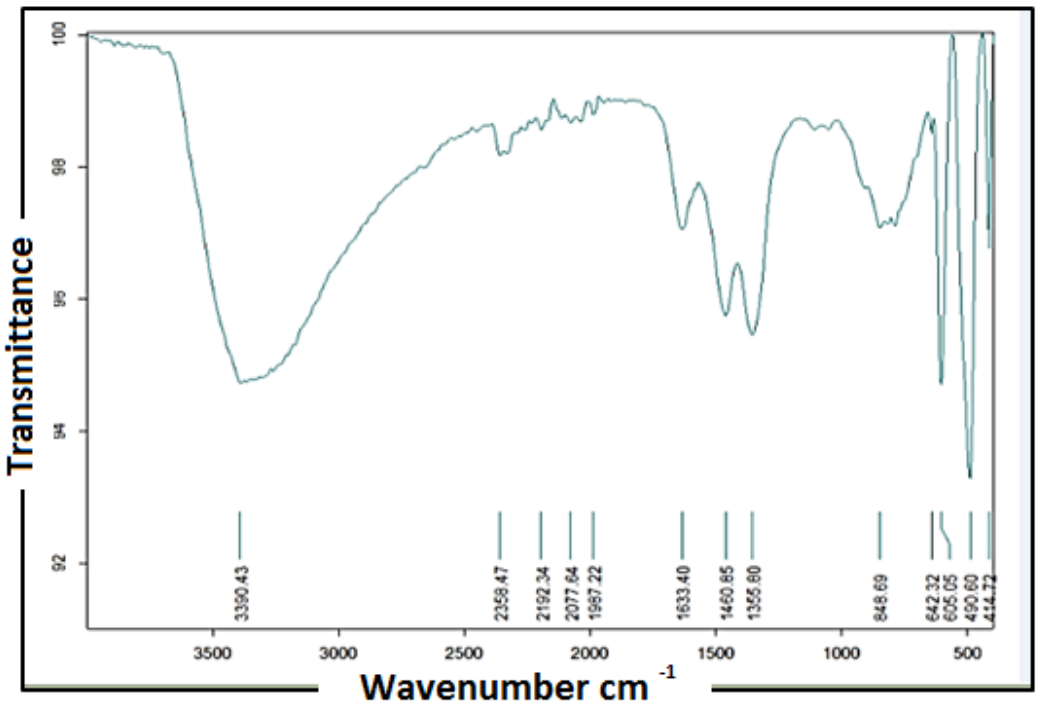

Figure S8: FTIR spectra of the CuO NPs